Parity restoration in the highly truncated diagonalization approach: Application to the outer fission barrier of ^{240}Pu

T. V. Nhan Hao,[1,2,3,*] P. Quentin,[2,3] and L. Bonneau[2,3]
[1]*Tan Tao University, Tan Tao University Avenue, Tan Duc Ecity, Long An Province, Vietnam*
[2]*University of Bordeaux, CENBG, UMR5797, F-33170, Gradignan, France*
[3]*CNRS, IN2P3, CENBG, UMR5797, F-33170, Gradignan, France*
(Received 10 September 2012; published 10 December 2012)

The restoration of parity symmetry has been performed in the framework of the highly truncated diagonalization approach, which is suited to treat correlations in an explicitly particle-number-conserving microscopic approach. To do so we have assumed axial symmetry and used a generalized Wick's theorem attributable to Löwdin in a projection-after-variation scheme. We have chosen the Skyrme SkM* energy-density functional for the particle-hole channel and a density-independent δ force for the residual interaction. We have applied this approach in the region of the outer fission barrier of the ^{240}Pu nucleus. As a result, we have shown that the $K^\pi = 0^+$ fission isomeric state is statically unstable against intrinsic parity-breaking modes, while the projection does not affect the energy at the top of the intrinsic outer fission barrier. Altogether, this leads to an increase of the height of the outer fission barrier, with respect to the fission isomeric state, by about 350 keV, thus affecting significantly the spontaneous-fission half-life of the considered fission isomer.

DOI: 10.1103/PhysRevC.86.064307 PACS number(s): 21.60.Jz, 21.60.Cs, 24.10.Cn, 25.85.−w

I. INTRODUCTION

It has long been recognized that the second fission barriers of heavy nuclei are asymmetric under left-right reflection (or intrinsic-parity) symmetry [1]. Early self-consistent calculations [2] allowing violation of this symmetry have demonstrated that the height of the second fission barrier of actinide nuclei could be substantially reduced in that way. This has been confirmed in many further calculations (see, e.g., Ref. [3] using the Hartree-Fock + BCS approach). This phenomenon is driven by the heavy fragment shell effects, which explain [1], even at this early stage of the fission process, the asymmetric pattern of the fragment mass yields (at low compound-nucleus energy) that had been observed in this region.

In most microscopic or macro-microscopic calculations in the uranium and plutonium regions, upon increasing the elongation after the fission isomeric state, the intrinsic equilibrium solution becomes unstable with respect to the left-right reflection symmetry and acquires rapidly a larger octupole deformation, which is stabilized at a value corresponding to the most probable fragmentation, as previously noted. Yet, even though the intrinsic parity may be broken within some auxiliary microscopic solutions under consideration, the parity of the physical solution must be conserved during the fission process. For instance, if one describes the spontaneous fission of an even-even fissioning nucleus such as ^{240}Pu, one should evaluate the fission barrier obtained upon projecting intrinsic solutions onto the desired parity.

The highly truncated diagonalization approach (HTDA) is designed to produce realistic correlated wave functions in an approach that conserves explicitly the particle number and does not violate the Pauli principle [4]. While our approach takes stock of state-of-the-art energy-density functionals to describe microscopically mean-field properties, it had been initiated long before in simpler terms by various groups (see, e.g., Refs. [5–7]). The aim of this paper is to present an application of this HTDA method in a projected-after-variation calculation of the second fission barrier of ^{240}Pu, where the octupole deformation mode plays a very important role. It should be noted that very few microscopic calculations of fission barriers with parity-symmetry restoration have been performed so far. Among these calculations one can emphasize the systematic study of fission barriers carried out by Samyn and collaborators [8] within the Skyrme-Hartree-Fock-Bogolyubov approach with separate particle-number and parity projections using the BSk8 parametrization.

This paper is organized as follows. In Sec. II, a detailed presentation of the HTDA formalism and some of its key aspects are given. The analysis of the numerical results is presented in Sec. III. In the last section, the main results are summarized and some conclusions are drawn.

II. THEORETICAL FRAMEWORK

A. The highly truncated diagonalization approach

First let us briefly recall some general features of the HTDA approach, which allows treatment of various correlations, including pairing correlations, on the same footing in an explicitly particle-number-conserving approach as discussed in Refs. [4,9–12]. In the next section, the modifications to this standard approach, due to the projection method introduced in this paper, are discussed in detail.

We start from the Hamiltonian

$$\hat{H} = \hat{K} + \hat{V}, \tag{1}$$

where $\hat{K}$ is the kinetic energy and $\hat{V}$ is a two-body interaction. The latter may be density dependent, as is the case for the Gogny or the Skyrme interactions, and it includes the

*hao.tran@ttu.edu.vn

proton-proton Coulomb interaction. Insofar as the exchange term of the latter interaction is treated within the Slater approximation, as is generally performed in practice, some further spurious density dependence is included. For the sake of simplicity, we skip first the density dependence of $\hat{V}$, the effect of which in practice is discussed later.

We introduce an *a priori* arbitrary one-body potential $\hat{U}$. Of course, we try to implement all that is possible to incorporate in terms of guessed one-body properties of the correlated wave function in this auxiliary mean field (generally through some simplified self-consistent approach). We then introduce the corresponding auxiliary one-body Hamiltonian

$$\hat{H}_0 = \hat{K} + \hat{U} \tag{2}$$

and its lowest-energy eigenstate $|\Phi_0\rangle$, which is a Slater determinant corresponding to a quasiparticle vacuum of particle-hole type. In the following, we consider particle-hole excitations on this vacuum and define normal products in terms of the related quasiparticle operators.

Now we rewrite the original microscopic Hamiltonian as

$$\hat{H} = \hat{H}_{\rm IQP} + \hat{V}_{\rm res} + \langle\Phi_0|\hat{H}|\Phi_0\rangle, \tag{3}$$

where the independent quasiparticle Hamiltonian $\hat{H}_{\rm IQP}$ and the residual interaction $\hat{V}_{\rm res}$ are defined by

$$\hat{H}_{\rm IQP} = \hat{H}_0 - \langle\Phi_0|\hat{H}_0|\Phi_0\rangle, \tag{4}$$

$$\hat{V}_{\rm res} = (\hat{V} - \hat{U}) - \langle\Phi_0|(\hat{V} - \hat{U})|\Phi_0\rangle, \tag{5}$$

and we use the normal product $:\hat{A}:$ of an operator $\hat{A}$ with respect to the reference Slater determinant $|\Phi_0\rangle$. We recall that $:\hat{A}:$ is the rearranged product of creation followed by annihilation quasiparticle operators in $\hat{A}$ (of particle-hole type with respect to $|\Phi_0\rangle$), with a phase factor equal to the parity of the corresponding permutation. The Wick theorem applied to one- and two-body operators such as $\hat{U}$ and $\hat{V}$, respectively, implies that

$$\hat{U} = :\hat{U}: + \langle\Phi_0|\hat{U}|\Phi_0\rangle, \tag{6}$$

$$\hat{V} = :\hat{V}: + :\overline{V}: + \langle\Phi_0|\hat{V}|\Phi_0\rangle, \tag{7}$$

where $\overline{V}$ denotes the one-body reduction of $\hat{V}$ for the particle-hole vacuum $|\Phi_0\rangle$, defined by $\overline{V} = {\rm Tr}(\rho\widetilde{V})$, where ρ is the one-body density matrix associated with $|\Phi_0\rangle$ and $\widetilde{V}$ is the antisymmetrized version of the interaction $\hat{V}$. Consequently one has

$$\hat{H}_{\rm IQP} = :\hat{H}_0:, \tag{8}$$

$$\hat{V}_{\rm res} = :\hat{V}: + :\overline{V} - \hat{U}: . \tag{9}$$

Assuming that $\hat{V}$ and $\hat{U}$ reasonably produce similar descriptions of one-body properties of the studied nuclear system, we neglect the $:\overline{V} - \hat{U}:$ term.

In what follows, we use for $\hat{V}$ a Skyrme nucleon-nucleon effective interaction (adding of course the Coulomb interaction). As is well known, however, most of the parametrizations of such forces are not suited to treat correctly pairing correlations, with some noticeable exceptions, for example, in the parametrization SkP of Ref. [13] and SGII of Ref. [14]. In order to correct this deficiency, one replaces the two-body interaction $\hat{V}$ that appears in the definition (9) of $\hat{V}_{\rm res}$ by a zero-range interaction $\hat{V}_\delta$ as is usual for the description of such nuclear correlations. We choose it to be density independent since the *ad hoc* introduction here of a specific surface dependence is neither theoretically ascertained nor phenomenologically justified. Specifically, while the Skyrme force is used in the particle-hole channel (in $\hat{H}_{\rm IQP}$ and to evaluate $\langle\Phi_0|\hat{H}|\Phi_0\rangle$), the δ force is used for the particle-particle (and hole-hole) channel. In practice one thus approximates $\hat{V}_{\rm res}$ by

$$\hat{V}_{\rm res} \approx \hat{V}_\delta - :\overline{V}_\delta: - \langle\Phi_0|\hat{V}_\delta|\Phi_0\rangle, \tag{10}$$

where $\overline{V}_\delta$ is the one-body reduction of the $\hat{V}_\delta$ interaction for the particle-hole vacuum $|\Phi_0\rangle$.

Note that the above replacement of the two-body interaction introduces some state dependence of the Hamiltonian. In fact, introducing such an unwanted feature is unfortunately common, already at the Hartree-Fock level, in the current state-of-the-art microscopic treatments of nuclear properties when using Gogny or Skyrme energy-density functionals. The relevance of such a seemingly dubious approach should be ultimately validated, as usual, by the phenomenological quality of the obtained results.

The Hamiltonian (3) is diagonalized in the orthonormal many-body basis which includes the particle-hole vacuum $|\Phi_0\rangle$ and n-particle–n-hole (npnh) excitations with respect to $|\Phi_0\rangle$, generically noted $|\Phi_n\rangle$, with n ranging from 1 to some maximum order m. The correlated ground state can thus be written as

$$|\Psi\rangle = \chi_0\,|\Phi_0\rangle + \sum_{n=1}^{m}\sum_i \chi_n^{(i)}\left|\Phi_n^{(i)}\right\rangle, \tag{11}$$

where i distinguishes the various npnh configurations.

A satisfactory HTDA description of pairing correlations in heavy stable nuclei has been generally obtained with a many-body basis involving the particle-hole vacuum $|\Phi_0\rangle$ and pair excitations only. In this context, the Cooper pairs imply strictly time-reversed states, so that they have in particular the same charge. This approach deals then with the so-called $|T_z| = 1$ or nn, pp pairing correlations, an approach that is relevant far from the $N = Z$ line. In contrast, the np pairing correlations are important when studying nuclei near the $N = Z$ line (see, e.g., a recent thorough study in Ref. [15] within the HTDA framework).

Given the two approximations that have been made in $\hat{V}_{\rm res}$ (regarding $:\overline{V} - \hat{U}:$ and $:\hat{V}:$), the effect of including density-dependent parts in the two-body interaction is limited to the evaluation of $\langle\Phi_0|\hat{H}|\Phi_0\rangle$, where they have been fully taken into account.

B. Projected energy

The state $|\Psi_p\rangle$ of definite parity $p = \pm 1$ is obtained by the action of the parity projection operator $\hat{P}_p = \frac{1}{2}(1 + p\,\hat{\Pi})$, where $\hat{\Pi}$ denotes the parity operator, onto the correlated (left-right asymmetrical) state $|\Psi\rangle$

$$|\Psi_p\rangle = N_p\hat{P}_p|\Psi\rangle, \tag{12}$$

where N_p is a real normalization constant defined by

$$N_p = \sqrt{2}\,(1 + p\,\langle\Psi|\hat{\Pi}|\Psi\rangle)^{-\frac{1}{2}}\,. \tag{13}$$

The resulting projected energy $E^{(p)} = \langle\Psi_p|\hat{H}|\Psi_p\rangle$ thus takes the form

$$E^{(p)} = \frac{\langle\Psi|\hat{H}|\Psi\rangle + \langle\widetilde{\Psi}|\hat{H}|\widetilde{\Psi}\rangle + p\,(\langle\Psi|\hat{H}|\widetilde{\Psi}\rangle + \langle\widetilde{\Psi}|\hat{H}|\Psi\rangle)}{2(1 + p\,\langle\Psi|\widetilde{\Psi}\rangle)}, \tag{14}$$

with $|\widetilde{\Psi}\rangle = \hat{\Pi}|\Psi\rangle$.

The Hamiltonian $\hat{H}$, including a density-dependent effective interaction, breaks the parity symmetry as long as the density does break it. So it seems contradictory to restore a symmetry for eigensolutions of a Hamiltonian that also breaks this specific symmetry. Such a feature, of course, is not related or restricted to the HTDA approach but is a consequence of the use of solution-dependent Hamiltonians as we have seen above when using, for example, Skyrme or Gogny energy-density functionals. Moreover, the calculation of $E^{(p)}$ is rather involved, since it requires calculation of four matrix elements together with one overlap. For these two reasons, we have chosen here to make some simplifying assumptions on the Hamiltonian and overlap kernels as explained in the next subsection.

C. Approximate Hamiltonian and overlap kernels

In principle, there is a total arbitrariness in choosing the one-body potential $\hat{U}$ to be introduced in the HTDA Hamiltonian. However, our solution of the secular equation is expanded in a truncated basis spanned by a subset of A-particle Slater determinants. On the one hand, such a limitation is embodied by the so-called single-particle configuration space, which is the restricted set of eigenfunctions of the one-body Hamiltonian $\hat{H}_0$ used to define particle and hole states. On the other hand, the many-body configuration space is restricted, beyond the quasiparticle vacuum $|\Phi_0\rangle$, to one-pair excitations with respect to $|\Phi_0\rangle$ written with a transparent notation as

$$|\Phi_2\rangle = a^\dagger_{k'}a^\dagger_{\bar{k}'}a_{\bar{k}}a_k|\Phi_0\rangle. \tag{15}$$

As a result our effective Hamiltonian does depend on the choice of the one-body potential $\hat{U}$.

Another $\hat{U}$ dependence of the Hamiltonian stems from the replacement of the Skyrme two-body interaction by a δ force in the definition of the residual interaction $\hat{V}_{\rm res}$. The one-body reduction of $\hat{V} - \hat{V}_\delta$ with respect to the particle-hole vacuum state $|\Phi_0\rangle$ depends by definition on this state and then ultimately on the potential $\hat{U}$. Similarly this replacement induces a $\hat{U}$ dependence of the expectation value of $\hat{V} - \hat{V}_\delta$ for $|\Phi_0\rangle$.

If the Hamiltonian were truly independent of the single-particle potential $\hat{U}$, we would have the freedom of choosing $\hat{U}$ according to the type of matrix elements involved in the calculation of $E^{(p)}$. Indeed, $\hat{U}$ does not have to assume a unique functional form and can be defined in a piecewise way in the one-body configuration space. Because of the above discussed limitations, doing so becomes an approximation. We explain below what choice we make to evaluate the Hamiltonian and overlap kernels.

1. Diagonal terms of the Hamiltonian kernel

The matrix element $\langle\Psi|\hat{H}|\Psi\rangle$ is encountered in usual HTDA calculations. To calculate the contribution from $\hat{H}_{\rm IQP}$, we choose the one-body potential $\hat{U}$ as the one-body reduction of $\hat{V}$ associated with the particle-hole vacuum $|\Phi_0\rangle$.

In the case of the matrix element $\langle\widetilde{\Psi}|\hat{H}|\widetilde{\Psi}\rangle$, we replace the above potential $\hat{U}$ with the parity-transformed operator $\widetilde{U}$ defined by

$$\widetilde{U} = \hat{\Pi}\hat{U}\hat{\Pi}\,. \tag{16}$$

The corresponding particle-hole vacuum is thus nothing but the mirror image $|\widetilde{\Phi}_0\rangle = \hat{\Pi}|\Phi_0\rangle$ of the particle-hole vacuum $|\Phi_0\rangle$ involved in the calculation of $\langle\Psi|\hat{H}|\Psi\rangle$. Then the one-body reduction of $\hat{V}_\delta$ for $|\widetilde{\Phi}_0\rangle$ is the parity-transformed operator $\widetilde{\overline{V}}_\delta = \hat{\Pi}\overline{V}_\delta\hat{\Pi}$. The resulting $\hat{V}_{\rm res}$ operator takes the form $\hat{V}_{\rm res} = \hat{V}_\delta - :\widetilde{\overline{V}}_\delta: - \langle\widetilde{\Phi}_0|\hat{V}_\delta|\widetilde{\Phi}_0\rangle$, and the corresponding HTDA Hamiltonian $\widetilde{H}$ is thus simply related to the previous Hamiltonian by a parity transformation. Owing to the unitary character of $\hat{\Pi}$ one thus obtains

$$\langle\widetilde{\Psi}|\widetilde{H}|\widetilde{\Psi}\rangle = \langle\Psi|\hat{H}|\Psi\rangle. \tag{17}$$

2. Off-diagonal terms of the Hamiltonian kernel

The off-diagonal matrix elements $\langle\Psi|\hat{H}|\widetilde{\Psi}\rangle$ and $\langle\widetilde{\Psi}|\hat{H}|\Psi\rangle$ are numerically difficult to evaluate, especially in the context of the previously discussed state dependence of the Hamiltonian.

First of all, by making a judicious choice of the arbitrary one-body potential $\hat{U}$ entering the definition of the HTDA Hamiltonian, it is possible in general to equate the two matrix elements $\langle\Psi|\hat{H}|\widetilde{\Psi}\rangle$ and $\langle\widetilde{\Psi}|\widetilde{H}|\Psi\rangle$. For that it suffices to choose $\widetilde{U}$ and the resulting particle-hole vacuum $|\widetilde{\Phi}_0\rangle$, similar to what has been discussed for the diagonal term $\langle\widetilde{\Psi}|\hat{H}|\widetilde{\Psi}\rangle$. Taking advantage of the arbitrariness of the auxiliary one-body potential used to define the HTDA Hamiltonian, one may decide to consider the Hamiltonian $\widetilde{H}$ for matrix elements between the bra $\langle\Psi|$ and the ket $|\widetilde{\Psi}\rangle$, while using the Hamiltonian $\hat{H}$ for matrix elements between the bra $\langle\widetilde{\Psi}|$ and the ket $|\Psi\rangle$.

Actually, we have performed a further approximation, prompted by two motivations. First, as already noted, we introduce in practice through our approximate diagonalization process a spurious dependence of the Hamiltonian of the auxiliary one-body potential $\hat{U}$. This makes the above choice somewhat arbitrary. Second, we face here the problem usually encountered in configuration-mixing calculations using state-dependent Hamiltonians. It concerns, as is well known, the choice of the reference state defining this Hamiltonian when computing nondiagonal matrix elements (where *nondiagonal* refers here to different reference states). One could think of using the one-body reduction of the underlying two-body interaction with respect to the mixed density in the sense of, for example, Ref. [16], but in practice it so happens that the

non-negative character of the corresponding local density (its matrix elements that are diagonal in **r** space) is not always warranted. This entails, of course, a problem to define the density-dependent part of the Skyrme mean field and the Slater Coulomb exchange mean field. These fields involve, often for the former and surely for the latter, a noninteger power of the density. Moreover, let us state again that it does not seem fully satisfactory, *a priori*, to use an auxiliary Hamiltonian, breaking some symmetry in the process of restoring this symmetry, for its solution.

This is why we have made further use of the arbitrariness of the one-body operator $\hat{U}$ as follows. For a given intrinsic solution in the collective deformation space as specified, for example, by its axial quadrupole Q_{20} and octupole Q_{30} moments, we define the potential $\hat{U}$ in the HTDA Hamiltonian as the one corresponding to the parity-symmetrical vacuum solution ($Q_{30} = 0$) with the same value of the axial quadrupole moment.

In that case, since the two Hamiltonians $\hat{H}$ and $\widetilde{H}$ are trivially identical, one gets

$$\langle\Psi|\hat{H}|\widetilde{\Psi}\rangle = \langle\widetilde{\Psi}|\hat{H}|\Psi\rangle, \tag{18}$$

and since these matrix elements are real, we deduce that the HTDA Hamiltonian is indeed Hermitian.

Using Eqs. (17) and (18), we can rewrite the projected energy (14) as

$$E^{(p)} = \frac{\langle\Psi|\hat{H}|\Psi\rangle + p\langle\Psi|\hat{H}|\widetilde{\Psi}\rangle}{1 + p\,\langle\Psi|\widetilde{\Psi}\rangle}. \tag{19}$$

To compute the matrix elements involving bras $\langle\Psi|$ and kets $|\widetilde{\Psi}\rangle$, we take stock of the fact that we have to deal with matrix elements between Slater determinants. It is thus more appropriate to use the Löwdin approach of Ref. [17] than the Balian-Brezin generalized Wick theorem [18]. Let us denote by $|\Phi\rangle$ and $|\Phi'\rangle$ two Slater determinants built from single-particle states generically noted $|\phi_k\rangle$ and $|\phi'_l\rangle$, respectively, and by **d** the corresponding overlap matrix. By definition the elements d_{kl} of the overlap matrix are the overlaps $\langle\phi_k|\phi'_l\rangle$ of the occupied states $|\phi_k\rangle$ of the Slater determinant $|\Phi\rangle$ with the occupied states $|\phi'_l\rangle$ of $|\Phi'\rangle$. Then the matrix elements of a one-body operator $\hat{V}_1$ and a two-body operator $\hat{V}_2$ between $|\Phi\rangle$ and $|\Phi'\rangle$ are given by [17]

$$\langle\Phi|\hat{V}_1|\Phi'\rangle = \sum_{\substack{k\in\Phi\\ l\in\Phi'}} (-1)^{k+l}\langle\phi_k|\hat{V}_1|\phi'_l\rangle\, D_{\Phi\Phi'}(k|l), \tag{20}$$

$$\langle\Phi|\hat{V}_2|\Phi'\rangle = \frac{1}{2}\sum_{\substack{k_1\neq k_2\in\Phi\\ l_1\neq l_2\in\Phi'}} (-1)^{k_1+k_2+l_1+l_2}\langle\phi_{k_1}\phi_{k_2}|\hat{V}_2|\phi'_{l_1}\phi'_{l_2}\rangle \times D_{\Phi\Phi'}(k_1k_2|l_1l_2), \tag{21}$$

where the sums run over the occupied states of the Slater determinants and $D_{\Phi\Phi'}(k_1\ldots k_n|l_1\ldots l_n)$ is the minor of order n of the overlap matrix associated with the lines $k_1,\ldots,k_n$ and columns $l_1,\ldots,l_n$ (i.e., the determinant of the submatrix obtained by removing the lines $k_1,\ldots,k_n$ and columns $l_1,\ldots,l_n$ from the overlap matrix).

3. *Overlap kernel*

Within the HTDA framework, the overlap $\langle\Psi|\widetilde{\Psi}\rangle$ can be decomposed as

$$\begin{aligned}\langle\Psi|\widetilde{\Psi}\rangle = {}& \chi_0^2\langle\Phi_0|\widetilde{\Phi}_0\rangle + 2\chi_0\sum_{k=1}^{N-1}\chi_2^{(k)}\langle\Phi_0|\widetilde{\Phi}_2^{(k)}\rangle \\ & + 2\sum_{k=1}^{N-1}\sum_{l=1}^{k-1}\chi_2^{(k)}\chi_2^{(l)}\langle\Phi_2^{(k)}|\widetilde{\Phi}_2^{(l)}\rangle \\ & + \sum_{k=1}^{N-1}\left(\chi_2^{(k)}\right)^2\langle\Phi_2^{(k)}|\widetilde{\Phi}_2^{(k)}\rangle.\end{aligned} \tag{22}$$

The sums run over the $N-1$ one-pair configurations, where N is the size of the many-body basis.

As demonstrated by Löwdin [17], the overlap of any two Slater determinants $|\Phi\rangle$ and $|\Phi'\rangle$ can be expressed as the determinant of their overlap matrix **d**:

$$\langle\Phi|\Phi'\rangle = \det\mathbf{d}. \tag{23}$$

The time-reversal invariance of the $\hat{H}_{\rm IQP}$ Hamiltonian allows us to split the space of one-body states in two subspaces $\mathcal{E}$ and $\mathcal{E}^*$ deduced one from the other by time-reversal symmetry. Because of the axial symmetry we may define $\mathcal{E}$ as the subspace that incorporates all single-particle states $|\phi_i\rangle$ such that $\langle\phi_i|\hat{j}_z|\phi_i\rangle > 0$, where $\hat{j}_z$ is the projection of the total angular momentum operator on the symmetry axis chosen to be z here (we do not break axial symmetry). The matrix **d** can be written as a block-diagonal matrix defined as

$$\mathbf{d} = \begin{pmatrix} D & 0 \\ 0 & D^* \end{pmatrix}, \tag{24}$$

where D^* is the complex conjugate of the submatrix D, so that $\langle\Phi|\Phi'\rangle = |\det D|^2$. Moreover, since all the occupied states involved in D are eigenstates of the $\hat{j}_z$ operator with positive eigenvalues Ω_m (in $\hbar$ unit), the matrix D is block diagonal:

$$D = \begin{pmatrix} D_{\Omega_1} & 0 & \cdots & & \\ 0 & D_{\Omega_2} & 0 & \cdots & \\ \vdots & & \ddots & & \vdots \\ & & 0 & D_{\Omega_m} & 0 \\ & & & \cdots & 0 \end{pmatrix}, \tag{25}$$

where the zeros have to be understood as null submatrices and the submatrices $D_{\Omega_1},\ldots,D_{\Omega_m}$ correspond to Ω values for which the Slater determinants $|\Phi\rangle$ and $|\Phi'\rangle$ involve a finite number of occupied states with the quantum number Ω. If s_Ω (s'_Ω resp.) denotes the number of occupied states in $|\Phi\rangle$ ($|\Phi'\rangle$ resp.) with the eigenvalue Ω of the $\hat{j}_z$ operator, then the dimension of the submatrix D_Ω is the minimum of s_Ω and s'_Ω. If $s_\Omega \neq s'_\Omega$ the overlaps involving the occupied states of $|\Phi\rangle$ or $|\Phi'\rangle$, with the eigenvalue Ω, which do not appear in the submatrix D_Ω vanish and so does the determinant of D. Therefore, the nonvanishing overlaps $\langle\Phi|\Phi'\rangle$ are those for which $s_\Omega = s'_\Omega$ for all Ω values occurring in both $|\Phi\rangle$ and $|\Phi'\rangle$.

In this case, the overlap may be written as

$$\langle \Phi | \Phi' \rangle = \prod_m \left| \det D_{\Omega_m} \right|^2, \tag{26}$$

where the product runs over all positive values of Ω involved in $|\Phi\rangle$ and $|\Phi'\rangle$.

D. Some numerical aspects

The computational process that has been followed may be decomposed in three steps.

First we perform usual Hartree-Fock-plus-BCS (HF + BCS) calculations with a seniority force using an intrinsic parity-breaking code developed some years ago [3]. The SkM* [19] effective interaction is used. The strengths of the seniority force in the $T_z = 1$ and $T_z = -1$ channels only have been fixed [20] for the whole region of well-deformed nuclei, and a given size of the valence space in which the BCS equations are solved, so that neutron and proton odd-even binding-energy differences (for the ground states) are reasonably well reproduced. One must keep in mind that the particle-number nonconserving HF + BCS approach serves merely here to define relevant one-body auxiliary potentials $\hat{U}$.

In a second step, the strengths of the δ residual interaction in the $T_z = 1$ and $T_z = -1$ channels have been fixed for a given nucleus by relying on the phenomenological quality of our HF + BCS calculations (as hinted, e.g., from the reasonable results of Ref. [3] obtained for fission barrier heights). More specifically, we have chosen these strengths so as to reproduce the Fermi-surface diffuseness defined as $\mathrm{tr}[\hat{\rho}^{1/2}(1-\hat{\rho})^{1/2}]$, where $\hat{\rho}$ is the one-body reduced density matrix of the correlated wave function, obtained in HF + BCS calculations for both charge states. Since this fit depends, of course, on the choice of a deformation for the solution, we have arbitrarily applied this condition at one point in the deformation space that is of interest for the problem under scrutiny. In our case, we have chosen to make this fit at the second fission barrier of ^{240}Pu. The HTDA calculations have then been performed within a space defined

(i) by taking all single-particle states lying in a band of ±6 MeV around the proton and neutron Fermi energies in $|\Phi_0\rangle$ (defined as half the differences between the last occupied and the first unoccupied single-particle states) and
(ii) by taking all one-pair transfer states available from the previously defined single-particle valence space.

Finally, we have carried out a projection after variation of the obtained HTDA ground state and calculated the corresponding energy as described above.

III. RESULTS AND DISCUSSION

The main purpose of this paper is to study the impact of parity restoration on the outer fission barrier of ^{240}Pu when starting from a $K^\pi = 0^+$ state. This state is relevant for the induced fission of the $1/2^+$ ground state of ^{239}Pu by an s-wave neutron or the ground-state spontaneous-fission decay of the ^{240}Pu nucleus.

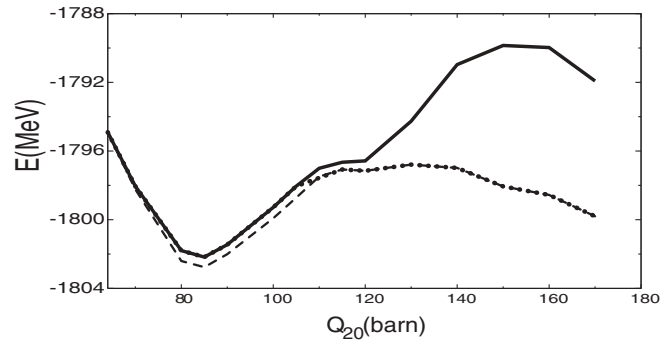

FIG. 1. Deformation energy curves from before the fission isomeric state and up to after the second barrier region of the ^{240}Pu nucleus. Three curves are plotted: for symmetrical HTDA solutions (solid curve), for asymmetrical HTDA solutions unprojected (dotted curve), and for projection on positive parity states (dashed curve).

To do so we have studied the relevant characteristics of the two-dimensional deformation energy surface for axial quadrupole and octupole deformations from before the fission isomeric state up to after the outer saddle point.

The results are summarized in Fig. 1. Throughout this paper, the specific definition of the multipole moments Q_{20}, Q_{30}, and Q_{40} is the one given, for example, in Ref. [21]. As is very well known (see in particular Ref. [3] where HF + BCS calculations have been performed for this nucleus making use of the same Skyrme interaction), allowing for a break of the left-right reflection symmetry considerably lowers the fission barrier down to values consistent with their experimental values. Consistently, we find in our HTDA calculations a value of 5.5 MeV for the second fission barrier height to be compared with the 5.1 MeV experimental value [22].

In that respect one should mention that the conclusion drawn from this seemingly very good success should be somewhat watered down, *a priori*, because these calculations do not take into account some corrections that would lower the fission barrier height (as the rotational energy correction, since we are merely calculating here a fission barrier for intrinsic states) and some others that would raise it. In the latter case, we mention, beyond the corrections related to the present work, those found in Refs. [23,24] and systematically explained in Ref. [24], which stem from the approximate treatment of the Coulomb exchange terms.

Let us first remark that upon projecting parity-breaking intrinsic solutions on positive-parity (negative-parity resp.) eigenstates, one always obtains projected energies equal to or lower (resp. higher) than the energies of the intrinsic solutions. The relative ordering of the two projected energies for the same intrinsic parity-breaking state may be hinted, if not demonstrated, by the following consideration, which is a quite general quantum mechanical result (see, e.g., Ref. [25]). If one were to mix, in a generator-coordinate method (GCM) fashion for instance, positive- and negative-parity states in the vicinity of the intrinsic equilibrium solution at a given value of Q_{20}, one would likely generate a zero-node solution in the Q_{30} direction for the lowest positive-parity state and a one-node solution for the lowest negative-parity state. One knows, for example, from the discussion of Ref. [25], that the former would correspond

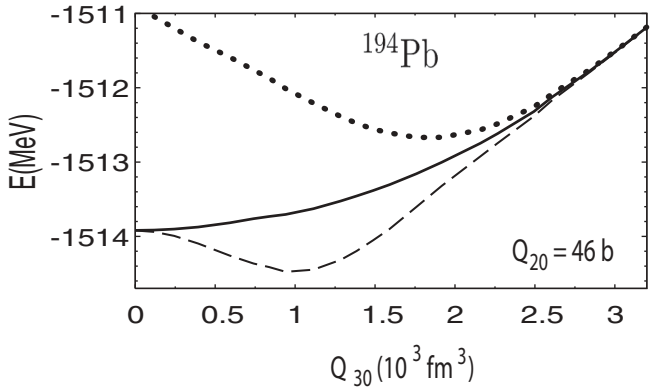

FIG. 2. Octupole deformation properties of ^{194}Pb for the superdeformed intrinsic state ($Q_{20} = 46$ b). Three curves are plotted: for asymmetrical unprojected HTDA solutions (solid curve), for projection on negative-parity states (dotted curve), and for projection on positive-parity states (dashed curve).

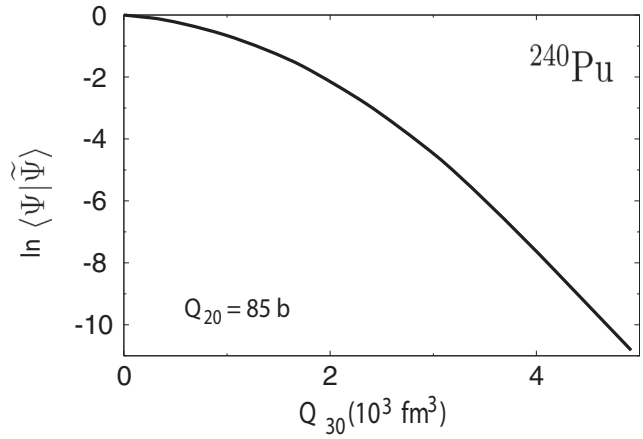

FIG. 3. Logarithm of the overlap $\langle\Psi|\tilde{\Psi}\rangle$ as a function of the octupole deformation at the elongation defined by $Q_{20} = 85$ b.

to the ground state (in such a nondegenerate case). The fact that positive-parity solutions (not mixed by the GCM ansatz) are lower in energy than the corresponding negative-parity solutions may be deemed as consistent with the above. Note also, *en passant*, that we have not made the effort to find out energies of negative-parity states in the vicinity of the reflection-symmetrical case, through cumbersome appropriate treatments of this limiting case, since we are merely interested here in the behavior of positive-parity solutions.

From the above discussion, one can expect four different behaviors of the positive-parity energy curve $E^{+}(Q_{30}, Q_{20}^{\text{fixed}})$:

(i) One has an equilibrium intrinsic solution that is symmetrical ($Q_{30} = 0$) with a large stiffness in the axial octupole mode so that the projection is not able to create a positive-parity minimum for a finite value of Q_{30}. Clearly, such a projection reduces the stiffness with respect to the axial octupole mode, possibly creating dynamical instability.

(ii) If, in contrast to (i), the symmetrical equilibrium solution has a sufficiently small stiffness, the parity projection can create a pocket for a nonvanishing value of the octupole moment. A static instability away from symmetry, which was not available with the intrinsic solutions, appears. This situation has been encountered in projected HF + BCS calculations for superdeformed solutions in the mercury-lead region [26]. It has also been found in our calculations of the superdeformed intrinsic state of ^{194}Pb as shown in Fig. 2.

(iii) This case is concerned with situations where the intrinsic equilibrium solution is not symmetrical but corresponds to a not-too-large absolute value of $|Q_{30}|$ [where the concept of large is defined in case (iv) below]. The positive-parity projection emphasizes the instability already present at the intrinsic level, yielding possible corresponding equilibrium $|Q_{30}|$ values, which may differ significantly from what has been obtained in the intrinsic case.

(iv) Beyond some critical value of $|Q_{30}|$, the overlap and Hamiltonian kernels between an intrinsic wave function and its parity transform become negligible, so that in the calculations of the projected energies according to Eq. (19) one obtains

$$E^{(p)} \approx E_{\text{intr}}, \tag{27}$$

where E_{intr} stands for the energy of the intrinsic solution $|\Psi\rangle$, namely $E_{\text{intr}} = \langle\Psi|\hat{H}|\Psi\rangle$.

This is exemplified in Fig. 3, where the overlap of a solution obtained for ^{240}Pu nucleus at $Q_{20} = 85$ b with parity-transformed wave function is plotted as a function of Q_{30}. The drop in the overlap to about 0.01 just above $Q_{30} \simeq 3.5$ b$^{3/2}$ is to be paralleled with the behavior of the energy curves shown in Fig. 5, where a clear convergence of the three energies E_{intr}, $E^{(+)}$, and $E^{(-)}$ is observed beyond this value of the axial octupole moment.

The consequence of this feature is that when the nonsymmetrical intrinsic equilibrium solution has a value of $|Q_{30}|$ larger than the above critical value of almost vanishing overlaps, then the projection is ineffective in producing any change in the equilibrium solution. One obtains a trivial twofold degeneracy corresponding to solutions which are connected by parity transformation. This situation has also been encountered in projected Hartree-Fock-Bogolyubov calculations with the Gogny energy-density functional for ^{222}Ra [27]. It has also been found in our calculations for this isotope as shown on Fig. 4.

As can be seen in Fig. 5, we are encountering the behaviors (i) to (iv) in this order in the study of the minimal-energy solutions obtained at a given Q_{20} value, when increasing it from after the first barrier up to beyond the second barrier. The transitions between these various patterns take place at $Q_{20} \simeq 65$, 105, and 125 b. Alternatively we have plotted in Fig. 6 the equilibrium (Q_{20}, Q_{30}) values for the intrinsic and positive-parity solutions. Clearly the onset of a stable axial octupole deformation takes place in the fission process much earlier for the projected solutions than for the intrinsic ones.

This entails two important consequences. First, this leads to the proposed existence of a stable octupole deformation for the fission isomeric state corresponding to $Q_{20} = 85$ b, $Q_{40} = 10.5$ b^2, and $Q_{30} = 4.9$ b$^{3/2}$. Second, this provides a systematic enhancement of the outer fission barrier with respect to the

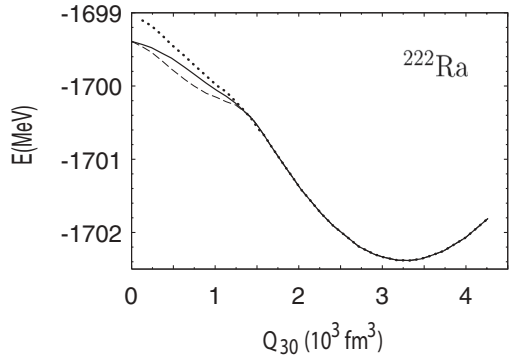

FIG. 4. Octupole deformation properties of ^{222}Ra at the ground state corresponding to $Q_{20} = 13$ b. Three curves are plotted: for asymmetrical unprojected HTDA solutions (solid curve), for projection on negative-parity states (dotted curve), and for projection on positive-parity states (dashed curve).

fission isomeric state. This enhancement is only due to the relatively soft character of the octupole deformation energy curve near the fission isomeric state since at the top of the second barrier the octupole deformation is too large to yield any projection effect.

It is our contention that these two consequences are quite general in the actinide region. Therefore, we deem that the outer (positive-parity) fission barrier heights with respect to the fission isomeric state are probably systematically

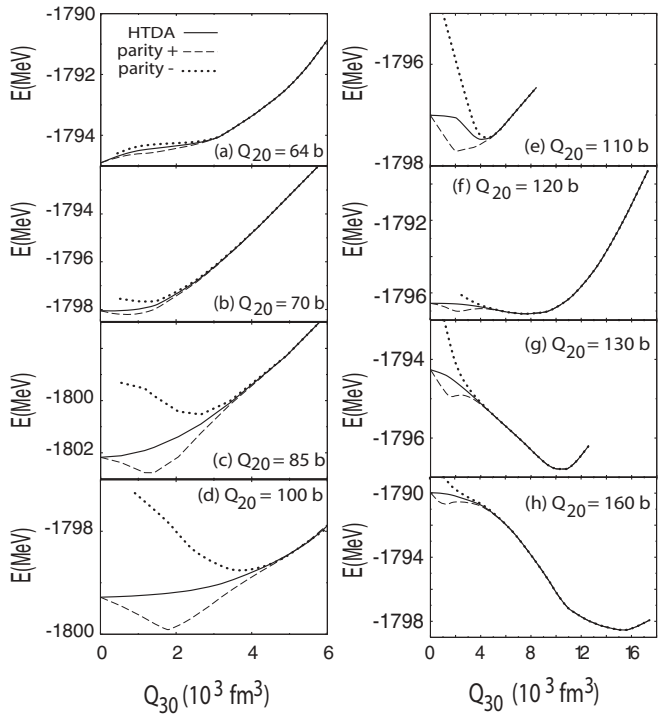

FIG. 5. Deformation energy curves for some values of the elongation (defined by Q_{20}) around the isomeric state and the second barrier region of the ^{240}Pu nucleus. Three curves are plotted: for asymmetrical unprojected HTDA solutions (solid curve), for the projection on the negative states (dotted curve), and for the projection on the positive states (dashed curve).

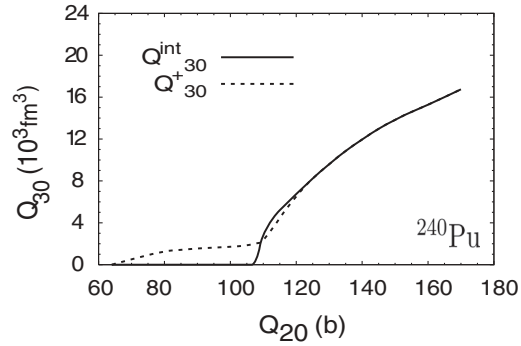

FIG. 6. The octupole deformation curves of the projection on the positive states and asymmetrical unprojected HTDA solutions (denoted alternatively by Q^{+}_{30} and $Q^{\rm int}_{30}$) as function of the quadrupole deformation Q_{20}.

underestimated in this region of nuclides, within unprojected calculations. In the present calculations, the enhancement of the fission barrier height amounts to about 350 keV for the state of the compound ^{240}Pu nucleus. As a well-known rule of thumb, a variation of 1 MeV in a few-MeV fission barrier height roughly corresponds to a change of the tunneling probability by four orders of magnitude. Thus, the effect of the parity projection obtained here cannot be considered as negligible for the penetrability of the outer barrier from the fission isomeric state.

IV. CONCLUSIONS

In this paper, we have investigated the outer fission barrier of ^{240}Pu within the microscopic HTDA approach and evaluated the effect of the parity projection on this barrier. The projection on positive-parity states around the fission isomeric state has demonstrated the instability of this state with respect to the Q_{30} mode. This confirms the results of Bonche *et al.* [28] and Egido and Robledo [27] obtained in another superdeformation region (superdeformed states in the Hg-Pb region). As is already well known from Möller and Nilsson [1], the fission valley when rising towards the outer barrier becomes more asymmetrical with respect to the intrinsic parity. Consequently, much before reaching the outer saddle point, one goes beyond the critical values where, for a given Q_{20} value, the matrix elements $\langle\Psi|\hat{O}|\tilde{\Psi}\rangle$ vanish (where $\hat{O}$ stands for the Hamiltonian or the identity operator). In this case, it is clear that projected and unprojected energies are similar. As a consequence of the isomeric-state instability, one expects that the positive-parity fission barrier height with respect to the fission isomeric state is larger than the unprojected one. Therefore, one may conclude that our results provide a hint for a systematic underestimation of the outer fission barrier height in usual unprojected calculations.

ACKNOWLEDGMENTS

Two of the authors (T.V.N.H. and P.Q.) acknowledge support by the France Vietnam Particle Physics Laboratory

(FV-PPL LIA) and by the National Foundation for Science and Technology Development (NAFOSTED) of Vietnam through Grant No. 103.04-2010.02. T.V.N.H. thanks the Saigon Institute for Computational Science and Technology (Saigon ICST) for the excellent working conditions extended to him.

[1] P. Möller and S. G. Nilsson, Phys. Lett. B **31**, 283 (1970).
[2] J. F. Berger, M. Girod, and D. Gogny, Nucl. Phys. A **428**, 23C (1984).
[3] L. Bonneau, P. Quentin, and D. Samsœn, Eur. Phys. J. A **21**, 391 (2004).
[4] N. Pillet, P. Quentin, and J. Libert, Nucl. Phys. A **697**, 141 (2002).
[5] J. Y. Zeng and T. S. Cheng, Nucl. Phys. A **405**, 1 (1983).
[6] M. Hasegawa and S. Tazaki, Phys. Rev. C **35**, 1508 (1987).
[7] O. Burglin and M. Rowley, Nucl. Phys. A **602**, 21 (1996).
[8] M. Samyn, S. Goriely, and J. M. Pearson, Phys. Rev. C **72**, 044316 (2005).
[9] P. Quentin, H. Naidja, L. Bonneau, J. Bartel, and T. L. Ha, Int. J. Mod. Phys. E **17**, 228 (2008).
[10] H. Naidja, P. Quentin, T. L. Ha, and D. Samsœn, Phys. Rev. C **81**, 044320 (2010).
[11] H. Lafchiev, J. Libert, P. Quentin, and T. L. Ha, Nucl. Phys. A **845**, 33 (2010).
[12] L. Bonneau, P. Quentin, and K. Sieja, Phys. Rev. C **76**, 014304 (2007).
[13] J. Dobaczewski, H. Flocard, and J. Treiner, Nucl. Phys. A **422**, 103 (1984).
[14] Nguyen Van Giai and H. Sagawa, Phys. Lett. B **106**, 379 (1981).
[15] J. Le Bloas, L. Bonneau, P. Quentin, J. Bartel, and D. D. Strottman, Phys. Rev. C **86**, 034332 (2012).
[16] P. Bonche, J. Dobaczewski, H. Flocard, P.-H. Heenen, and J. Meyer, Nucl. Phys. A **510**, 466 (1990).
[17] P. O. Löwdin, Phys. Rev. **97**, 1490 (1955).
[18] R. Balian and E. Brezin, Nuovo Cimento B **64**, 37 (1969).
[19] J. Bartel, P. Quentin, M. Brack, C. Guet, and H. B. Håkansson, Nucl. Phys. A **386**, 79 (1982).
[20] L. Bonneau, P. Quentin, and P. Möller, Phys. Rev. C **76**, 024320 (2007).
[21] L. Bonneau and P. Quentin, Phys. Rev. C **72**, 014311 (2005).
[22] S. Bjørnholm and J. Lynn, Rev. Mod. Phys. **52**, 725 (1980).
[23] M. Anguiano, J. L. Egido, and L. M. Robledo, Nucl. Phys. A **683**, 227 (2001).
[24] J. Le Bloas, M.-H. Koh, P. Quentin, L. Bonneau, and J. I. A. Ithnin, Phys. Rev. C **84**, 014310 (2011).
[25] R. Courant and D. Hilbert, *Methods of Mathematical Physics* (Interscience, New York, 1953), Sec. 6.6.
[26] P. Bonche, S. J. Krieger, M. S. Weiss, J. Dobaczewski, H. Flocard, and P.-H. Heenen, Phys. Rev. Lett. **66**, 876 (1991).
[27] J. L. Egido and L. M. Robledo, Nucl. Phys. A **524**, 87 (1991).
[28] P. Bonche, P.-H. Heenen, H. Flocard, and D. Vautherin, Phys. Lett. B **175**, 387 (1986).